

END
DATE
FILMED
2-81
DTIC

DDC FILE COPY

AD A094383

SECURITY CLASSIFICATION OF THIS PAGE (When Data Entered)

REPORT DOCUMENTATION PAGE		READ INSTRUCTIONS BEFORE COMPLETING FORM
1. REPORT NUMBER NRL Memorandum Report 4423	2. GOVT ACCESSION NO. AD-A094383	3. RECIPIENT'S CATALOG NUMBER
4. TITLE (and Subtitle) <u>A PARAMETRIC STUDY OF INTERSTELLAR HELIUM</u> <u>ATOMS INCIDENT UPON THE EARTH</u>		5. TYPE OF REPORT & PERIOD COVERED Interim report on a continuing NRL problem.
7. AUTHOR(s) R. R. Meier		6. PERFORMING ORG. REPORT NUMBER
9. PERFORMING ORGANIZATION NAME AND ADDRESS Naval Research Laboratory Washington, DC 20375		10. PROGRAM ELEMENT, PROJECT, TASK AREA & WORK UNIT NUMBERS 61153N; RR03406427 41-0939-0-1
11. CONTROLLING OFFICE NAME AND ADDRESS 14) NRL-MR-4423		12. REPORT DATE January 28, 1981
14. MONITORING AGENCY NAME & ADDRESS (if different from Controlling Office)		13. NUMBER OF PAGES 36
		15. SECURITY CLASS. (of this report) UNCLASSIFIED
		15a. DECLASSIFICATION/DOWNGRADING SCHEDULE
16. DISTRIBUTION STATEMENT (of this Report) Approved for public release; distribution unlimited.		
17. DISTRIBUTION STATEMENT (of the abstract entered in Block 20, if different from Report)		
18. SUPPLEMENTARY NOTES		
19. KEY WORDS (Continue on reverse side if necessary and identify by block number) Interstellar helium Precipitating atoms		
20. ABSTRACT (Continue on reverse side if necessary and identify by block number) Calculations of the intensity of interstellar helium atoms at earth orbit are made with a model which takes into account perturbation of the Maxwell-Boltzmann velocity distribution by solar gravity and photoionization loss. Seasonal sky maps are presented and assessments of the sensitivity of the intensity of atoms in the vicinity of the earth to the various parameters of the gas are given.		

DD FORM 1 JAN 73 1473

EDITION OF 1 NOV 65 IS OBSOLETE
S/N 0102-LF-014-6601

SECURITY CLASSIFICATION OF THIS PAGE (When Data Entered)

CONTENTS

I. INTRODUCTION	1
II. THE MODEL	2
III. INTENSITY PATTERNS	3
IV. DETERMINATION OF GAS PARAMETERS	26
V. SUMMARY	32
ACKNOWLEDGMENTS	33
REFERENCES	34

DTIC
ELECTE
S FEB 2 1981 D
B

Accession For	
ADIS CPA&I	<input checked="" type="checkbox"/>
ADIS TAD	<input type="checkbox"/>
ADIS TAD	<input type="checkbox"/>
Availability Codes	
Dist	Special
A	

A PARAMETRIC STUDY OF INTERSTELLAR HELIUM ATOMS
INCIDENT UPON THE EARTH

I. INTRODUCTION

Due to the relative motion of the solar system and the interstellar medium, neutral interstellar atoms can penetrate deep within the interplanetary regime. Studies of the backscatter of solar H Lyman α and He 584A radiation have demonstrated that it is possible to deduce information about the density, temperature, and velocity of such atoms from studies of the sky background radiation (see reviews by Holzer, 1977 and Thomas, 1978). However, additional observations to improve our knowledge of the local interstellar medium parameters are desirable to reduce uncertainties evident in the ranges of values determined by such methods.

One way to do this is to directly measure the intensity or flux per unit solid angle of interstellar atoms in the vicinity of the earth's orbit. Several groups are actively pursuing such programs with various experimental techniques. The purpose of this report is to provide theoretical models of atoms impacting the earth in an attempt to predict detailed characteristics of the atomic intensity pattern at 1 a.u. Atomic intensities are provided only for helium, as hydrogen is lost via charge exchange with the solar wind (and photoionization to a lesser extent) inside 2-6 a.u. from the sun.

Plots of the seasonal variation of the intensity and mean velocity are presented and the dependences upon the parameters of the

Manuscript submitted November 12, 1980.

interstellar gas and its interaction with the solar system are delineated. Recommendations are provided for the best times of year to obtain measurements of specific parameters.

II. THE MODEL

The intensity of atoms can be written as

$$I \text{ (atoms cm}^{-2} \text{ s}^{-1} \text{ sr}^{-1}) = \int_{v_m}^{\infty} |\underline{v} - \underline{v}_E| f(v) v^2 dv$$

where \underline{v}_E is the earth velocity vector in inertial coordinates (right ascension and declination), $|\underline{v} - \underline{v}_E|$ is the atomic velocity as seen in a coordinate system moving with the earth, v_m is the minimum allowable velocity (for an atom with zero velocity at infinity), and $f(v)$ is the velocity distribution, as perturbed by solar gravity, radiation pressure, and loss processes. The integration is carried out over the atomic velocity v in spherical velocity coordinates. Details of the model are given by Meier (1977) and are not repeated here.

The procedure for computing I first requires selection of the observation direction in order to determine the relative velocity, $\underline{v} - \underline{v}_E$. In stepping through the integration, knowledge of the observation direction and also the magnitude of the independent variable v permits computation of the relative velocity $|\underline{v} - \underline{v}_E|$ and the direction of \underline{v} , and finally the phase space distribution function f is evaluated. Gaussian quadratures are used for integration with as many as 32 ordinates for varying sub-intervals of v , depending upon the smoothness of the function. Limiting analytic solutions were evaluated (similar to those described by Meier, 1977) for comparison with results from the computer code.

In all cases the agreement was excellent. The present procedure represents a significant improvement over the approximate numerical technique used previously (Meier, 1977) for computing atomic intensities; the results presented herein are thus considerably more accurate.

III. INTENSITY PATTERNS

Figure 1 is a qualitative sketch showing typical trajectories of interstellar atoms moving through the solar system. Figure 2 shows a "standard" set of sky maps of the atomic helium intensity in right ascension and declination. The actual values of right ascension indicated on the upper horizontal axis of the plots apply to the character spaces below the zero of the "units" column of each number. Intensities are given for every 4° in α and 4° in δ . In each graph, the alpha-numeric character set is normalized to the maximum value of the intensity on that day (I_{\max}). The numerical value of the maximum is given at the bottom of the intensity plot and is indicated as an "E" character in the table just below. In the contour graph itself, the "E" has been replaced by an "+" for easy visual location. Each successive intensity grouping is lower than the next by $1/3$. Thus, on day 1 (Figure 2a), the character "D" represents all intensities between 1.88×10^5 and 2.51×10^5 atoms $\text{cm}^{-2} \text{ s}^{-1} \text{ sr}^{-1}$.

The mean velocity at each point is arbitrarily defined as

$$\bar{v} = \frac{\int |\underline{v} - \underline{v}_E| \left(\frac{dI}{dv} \right) dv}{I}$$

and is listed for I_{\max} just below the intensity plots. The total flux incident upon the earth, $\int I d\Omega$ is also given on the same line.

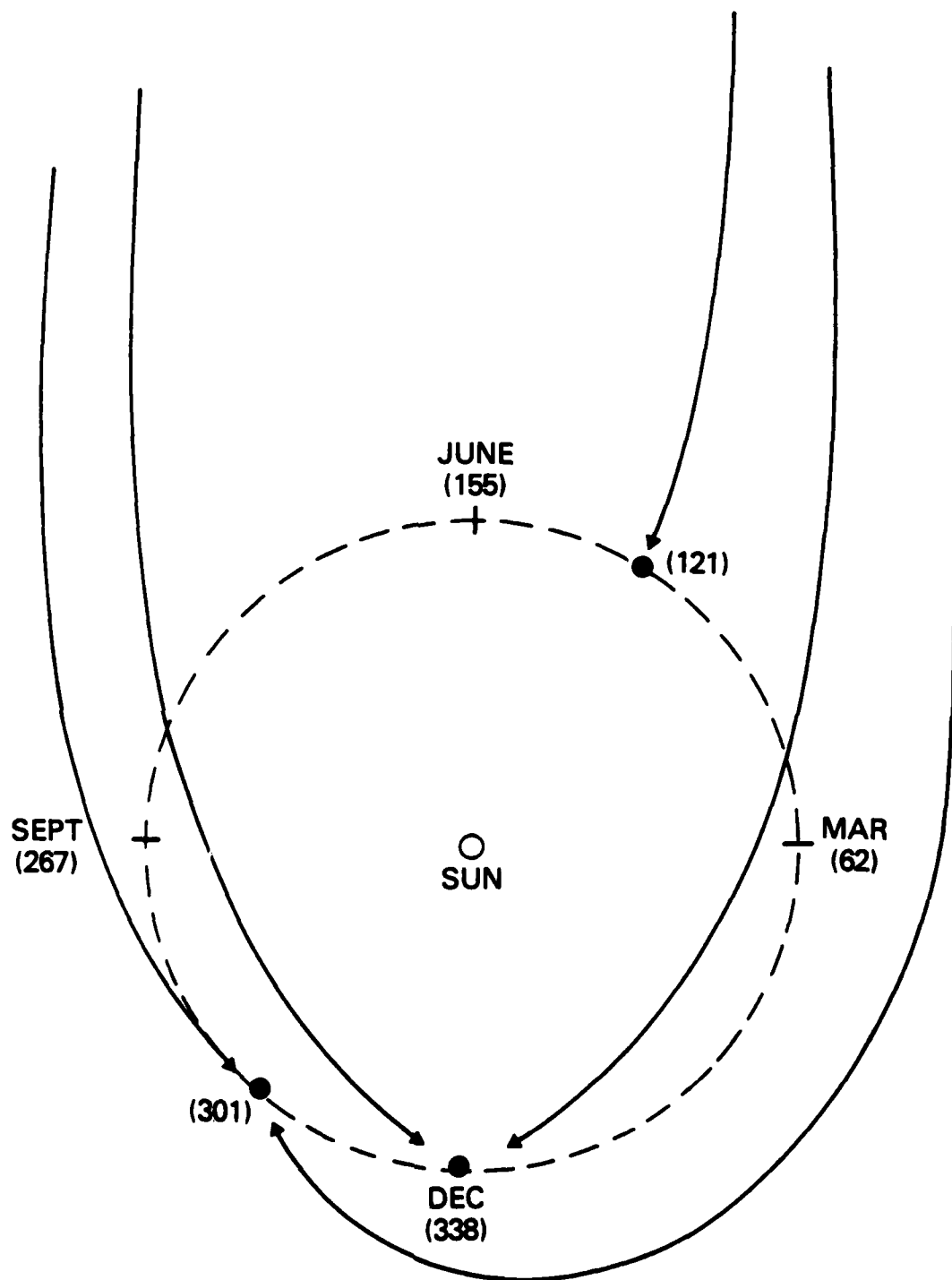
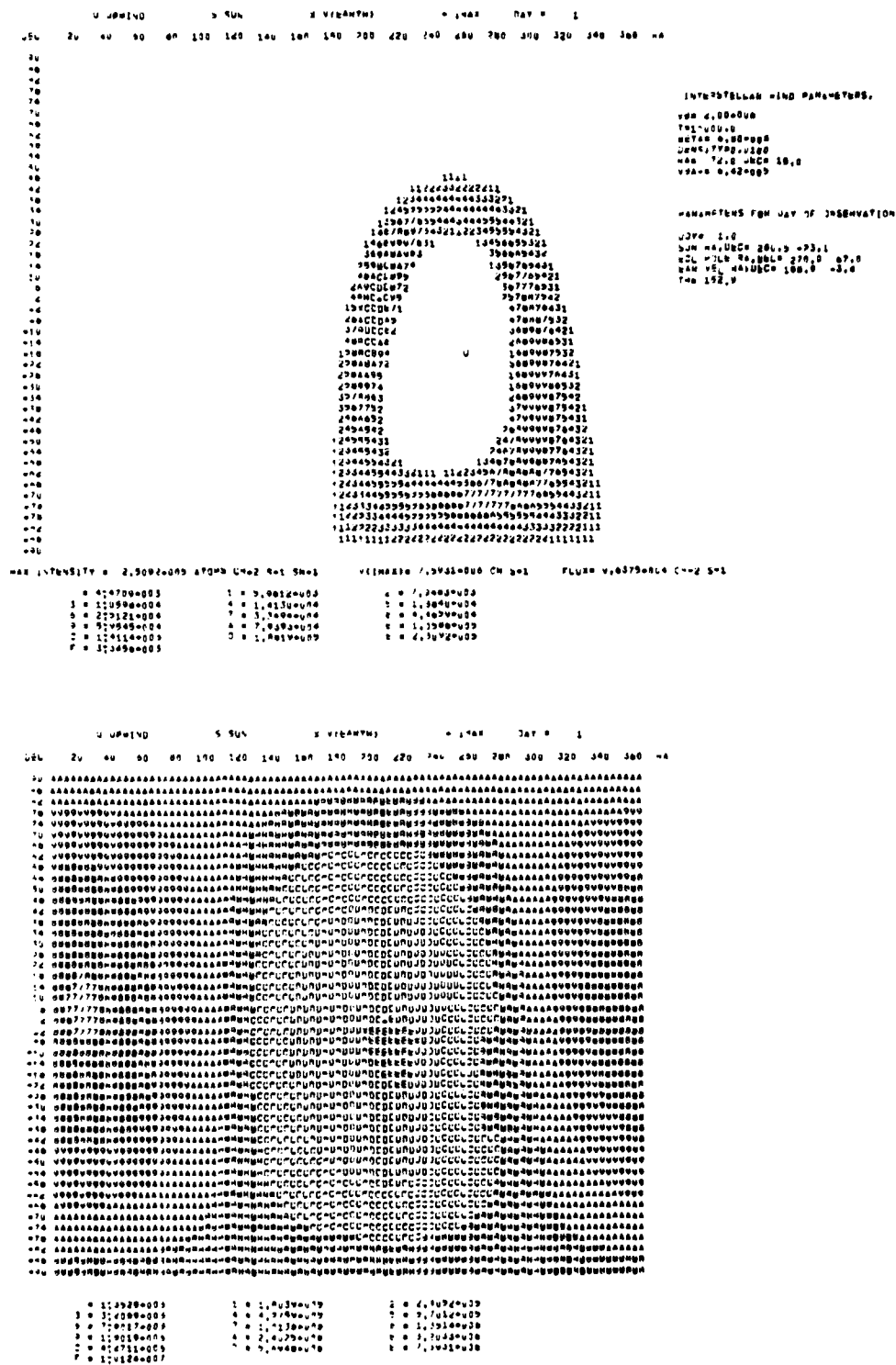


Fig. 1 — Sketch of orbits of interstellar helium atoms passing through solar system, projected into the ecliptic plane. The numbers in parentheses indicate the day-of-year for various positions of the earth and months when the earth is at closest approach to upwind, downwind, and 90° conditions.



0 17373=009	1 0 1,0810=09	2 0 0,13010=09
3 0 17401=009	4 0 0,13100=09	5 0 3,7490=09
6 0 7,9903=009	7 0 1,1490=00	8 0 1,1600=00
9 0 17920=009	1 0 2,4310=00	2 0 1,7009=00
3 0 3300=009	4 0 3,0700=00	5 0 7,1000=00
6 0 10220=009		

2370 21.0
 2374 40.0 202.2 -20.1
 2375 77.6 40.0 270.0 07.0
 2376 77.6 40.0 280.0 -1.3
 2377 132.7

6

```

      U JRMINU      S SUN      E VIGANTH      = 1.44E      DAY # 41
JEL 20 40 60 80 100 120 140 160 180 200 220 240 260 280 300 320 340 360 -A
+0
+2
+4
+6
+8
+10
+12
+14
+16
+18
+20
+22
+24
+26
+28
+30
+32
+34
+36
+38
+40
+42
+44
+46
+48
+50
+52
+54
+56
+58
+60
+62
+64
+66
+68
+70
+72
+74
+76
+78
+80
+82
+84
+86
+88
+90
+92
+94
+96
+98
+100

```

```

INTERSTELLAR WIND PARAMETERS
VW 4.00E+06
TSP-VWU-0
WETA 0.80E+00
WETA1 0.00E+00
WETA2 0.00E+00
WETA3 0.00E+00
WETA4 0.00E+00
WETA5 0.00E+00
WETA6 0.00E+00
WETA7 0.00E+00
WETA8 0.00E+00
WETA9 0.00E+00
WETA10 0.00E+00
WETA11 0.00E+00
WETA12 0.00E+00
WETA13 0.00E+00
WETA14 0.00E+00
WETA15 0.00E+00
WETA16 0.00E+00
WETA17 0.00E+00
WETA18 0.00E+00
WETA19 0.00E+00
WETA20 0.00E+00
WETA21 0.00E+00
WETA22 0.00E+00
WETA23 0.00E+00
WETA24 0.00E+00
WETA25 0.00E+00
WETA26 0.00E+00
WETA27 0.00E+00
WETA28 0.00E+00
WETA29 0.00E+00
WETA30 0.00E+00
WETA31 0.00E+00
WETA32 0.00E+00
WETA33 0.00E+00
WETA34 0.00E+00
WETA35 0.00E+00
WETA36 0.00E+00
WETA37 0.00E+00
WETA38 0.00E+00
WETA39 0.00E+00
WETA40 0.00E+00
WETA41 0.00E+00
WETA42 0.00E+00
WETA43 0.00E+00
WETA44 0.00E+00
WETA45 0.00E+00
WETA46 0.00E+00
WETA47 0.00E+00
WETA48 0.00E+00
WETA49 0.00E+00
WETA50 0.00E+00
WETA51 0.00E+00
WETA52 0.00E+00
WETA53 0.00E+00
WETA54 0.00E+00
WETA55 0.00E+00
WETA56 0.00E+00
WETA57 0.00E+00
WETA58 0.00E+00
WETA59 0.00E+00
WETA60 0.00E+00
WETA61 0.00E+00
WETA62 0.00E+00
WETA63 0.00E+00
WETA64 0.00E+00
WETA65 0.00E+00
WETA66 0.00E+00
WETA67 0.00E+00
WETA68 0.00E+00
WETA69 0.00E+00
WETA70 0.00E+00
WETA71 0.00E+00
WETA72 0.00E+00
WETA73 0.00E+00
WETA74 0.00E+00
WETA75 0.00E+00
WETA76 0.00E+00
WETA77 0.00E+00
WETA78 0.00E+00
WETA79 0.00E+00
WETA80 0.00E+00
WETA81 0.00E+00
WETA82 0.00E+00
WETA83 0.00E+00
WETA84 0.00E+00
WETA85 0.00E+00
WETA86 0.00E+00
WETA87 0.00E+00
WETA88 0.00E+00
WETA89 0.00E+00
WETA90 0.00E+00
WETA91 0.00E+00
WETA92 0.00E+00
WETA93 0.00E+00
WETA94 0.00E+00
WETA95 0.00E+00
WETA96 0.00E+00
WETA97 0.00E+00
WETA98 0.00E+00
WETA99 0.00E+00
WETA100 0.00E+00

```

```

PARAMETERS FROM DAY OF DISSEMINATION
DAY 41.0
SUN MA,UCP 322.7 -14.7
KUL MLE RA,DEL 270.0 07.1
KAM VEL 40,UCB 220.0 17.5
TWO 112.4

```

```

MAE LUTENSITY = 3.10E+005 ATOM C=2 C=1 SH=1
VIGANTH 1.04E+006 CM S=1
FLUX 3.50E+004 L=2 S=1

```

```

      U JRMINU      S SUN      E VIGANTH      = 1.44E      DAY # 41
JEL 20 40 60 80 100 120 140 160 180 200 220 240 260 280 300 320 340 360 -A
+0
+2
+4
+6
+8
+10
+12
+14
+16
+18
+20
+22
+24
+26
+28
+30
+32
+34
+36
+38
+40
+42
+44
+46
+48
+50
+52
+54
+56
+58
+60
+62
+64
+66
+68
+70
+72
+74
+76
+78
+80
+82
+84
+86
+88
+90
+92
+94
+96
+98
+100

```

```

+0 1.10E+005 1 1.10E+005 1 1.10E+005
+2 3.50E+005 4 4.10E+005 2 2.10E+005
+4 7.00E+005 8 8.20E+005 4 4.20E+005
+6 1.10E+006 12 1.20E+006 6 6.20E+005
+8 1.50E+006 16 1.60E+006 8 8.20E+005
+10 1.90E+006 20 2.00E+006 10 1.00E+006
+12 2.30E+006 24 2.40E+006 12 1.20E+006
+14 2.70E+006 28 2.80E+006 14 1.40E+006
+16 3.10E+006 32 3.20E+006 16 1.60E+006
+18 3.50E+006 36 3.60E+006 18 1.80E+006
+20 3.90E+006 40 4.00E+006 20 2.00E+006
+22 4.30E+006 44 4.40E+006 22 2.20E+006
+24 4.70E+006 48 4.80E+006 24 2.40E+006
+26 5.10E+006 52 5.20E+006 26 2.60E+006
+28 5.50E+006 56 5.60E+006 28 2.80E+006
+30 5.90E+006 60 6.00E+006 30 3.00E+006
+32 6.30E+006 64 6.40E+006 32 3.20E+006
+34 6.70E+006 68 6.80E+006 34 3.40E+006
+36 7.10E+006 72 7.20E+006 36 3.60E+006
+38 7.50E+006 76 7.60E+006 38 3.80E+006
+40 7.90E+006 80 8.00E+006 40 4.00E+006
+42 8.30E+006 84 8.40E+006 42 4.20E+006
+44 8.70E+006 88 8.80E+006 44 4.40E+006
+46 9.10E+006 92 9.20E+006 46 4.60E+006
+48 9.50E+006 96 9.60E+006 48 4.80E+006
+50 9.90E+006 100 1.00E+007 50 5.00E+006

```

Fig. 2 (Continued)

0370 41.0
 0374 40.0 UGCA 300.0 -7.5
 0376 40.0 UGCA 270.0 -9.0
 0378 40.0 UGCA 240.0 -91.0
 0380 32.5

0	1.3373+009	1	1.17831+009	6	2.1774+009
1	3.11899+009	4	0.2445+009	7	2.5378+009
2	7.7118+009	5	0.1180+009	8	1.1337+009
3	1.70811+009	4	2.1787+009	9	3.1800+009
4	0.74218+009	5	2.9484+009	0	7.2056+009

8


```

      J 000100      S 000      E 0000000      P 000      TAY 0 101
      2L 40 60 80 100 120 140 160 180 200 220 240 260 280 300 320 340 360 380 400 420 440 460 480 500 520 540 560 580 600 620 640 660 680 700 720 740 760 780 800 820 840 860 880 900 920 940 960 980 1000 1020 1040 1060 1080 1100 1120 1140 1160 1180 1200 1220 1240 1260 1280 1300 1320 1340 1360 1380 1400 1420 1440 1460 1480 1500 1520 1540 1560 1580 1600 1620 1640 1660 1680 1700 1720 1740 1760 1780 1800 1820 1840 1860 1880 1900 1920 1940 1960 1980 2000 2020 2040 2060 2080 2100 2120 2140 2160 2180 2200 2220 2240 2260 2280 2300 2320 2340 2360 2380 2400 2420 2440 2460 2480 2500 2520 2540 2560 2580 2600 2620 2640 2660 2680 2700 2720 2740 2760 2780 2800 2820 2840 2860 2880 2900 2920 2940 2960 2980 3000 3020 3040 3060 3080 3100 3120 3140 3160 3180 3200 3220 3240 3260 3280 3300 3320 3340 3360 3380 3400 3420 3440 3460 3480 3500 3520 3540 3560 3580 3600 3620 3640 3660 3680 3700 3720 3740 3760 3780 3800 3820 3840 3860 3880 3900 3920 3940 3960 3980 4000 4020 4040 4060 4080 4100 4120 4140 4160 4180 4200 4220 4240 4260 4280 4300 4320 4340 4360 4380 4400 4420 4440 4460 4480 4500 4520 4540 4560 4580 4600 4620 4640 4660 4680 4700 4720 4740 4760 4780 4800 4820 4840 4860 4880 4900 4920 4940 4960 4980 5000 5020 5040 5060 5080 5100 5120 5140 5160 5180 5200 5220 5240 5260 5280 5300 5320 5340 5360 5380 5400 5420 5440 5460 5480 5500 5520 5540 5560 5580 5600 5620 5640 5660 5680 5700 5720 5740 5760 5780 5800 5820 5840 5860 5880 5900 5920 5940 5960 5980 6000 6020 6040 6060 6080 6100 6120 6140 6160 6180 6200 6220 6240 6260 6280 6300 6320 6340 6360 6380 6400 6420 6440 6460 6480 6500 6520 6540 6560 6580 6600 6620 6640 6660 6680 6700 6720 6740 6760 6780 6800 6820 6840 6860 6880 6900 6920 6940 6960 6980 7000 7020 7040 7060 7080 7100 7120 7140 7160 7180 7200 7220 7240 7260 7280 7300 7320 7340 7360 7380 7400 7420 7440 7460 7480 7500 7520 7540 7560 7580 7600 7620 7640 7660 7680 7700 7720 7740 7760 7780 7800 7820 7840 7860 7880 7900 7920 7940 7960 7980 8000 8020 8040 8060 8080 8100 8120 8140 8160 8180 8200 8220 8240 8260 8280 8300 8320 8340 8360 8380 8400 8420 8440 8460 8480 8500 8520 8540 8560 8580 8600 8620 8640 8660 8680 8700 8720 8740 8760 8780 8800 8820 8840 8860 8880 8900 8920 8940 8960 8980 9000 9020 9040 9060 9080 9100 9120 9140 9160 9180 9200 9220 9240 9260 9280 9300 9320 9340 9360 9380 9400 9420 9440 9460 9480 9500 9520 9540 9560 9580 9600 9620 9640 9660 9680 9700 9720 9740 9760 9780 9800 9820 9840 9860 9880 9900 9920 9940 9960 9980 10000 10020 10040 10060 10080 10100 10120 10140 10160 10180 10200 10220 10240 10260 10280 10300 10320 10340 10360 10380 10400 10420 10440 10460 10480 10500 10520 10540 10560 10580 10600 10620 10640 10660 10680 10700 10720 10740 10760 10780 10800 10820 10840 10860 10880 10900 10920 10940 10960 10980 11000 11020 11040 11060 11080 11100 11120 11140 11160 11180 11200 11220 11240 11260 11280 11300 11320 11340 11360 11380 11400 11420 11440 11460 11480 11500 11520 11540 11560 11580 11600 11620 11640 11660 11680 11700 11720 11740 11760 11780 11800 11820 11840 11860 11880 11900 11920 11940 11960 11980 12000 12020 12040 12060 12080 12100 12120 12140 12160 12180 12200 12220 12240 12260 12280 12300 12320 12340 12360 12380 12400 12420 12440 12460 12480 12500 12520 12540 12560 12580 12600 12620 12640 12660 12680 12700 12720 12740 12760 12780 12800 12820 12840 12860 12880 12900 12920 12940 12960 12980 13000 13020 13040 13060 13080 13100 13120 13140 13160 13180 13200 13220 13240 13260 13280 13300 13320 13340 13360 13380 13400 13420 13440 13460 13480 13500 13520 13540 13560 13580 13600 13620 13640 13660 13680 13700 13720 13740 13760 13780 13800 13820 13840 13860 13880 13900 13920 13940 13960 13980 14000 14020 14040 14060 14080 14100 14120 14140 14160 14180 14200 14220 14240 14260 14280 14300 14320 14340 14360 14380 14400 14420 14440 14460 14480 14500 14520 14540 14560 14580 14600 14620 14640 14660 14680 14700 14720 14740 14760 14780 14800 14820 14840 14860 14880 14900 14920 14940 14960 14980 15000 15020 15040 15060 15080 15100 15120 15140 15160 15180 15200 15220 15240 15260 15280 15300 15320 15340 15360 15380 15400 15420 15440 15460 15480 15500 15520 15540 15560 15580 15600 15620 15640 15660 15680 15700 15720 15740 15760 15780 15800 15820 15840 15860 15880 15900 15920 15940 15960 15980 16000 16020 16040 16060 16080 16100 16120 16140 16160 16180 16200 16220 16240 16260 16280 16300 16320 16340 16360 16380 16400 16420 16440 16460 16480 16500 16520 16540 16560 16580 16600 16620 16640 16660 16680 16700 16720 16740 16760 16780 16800 16820 16840 16860 16880 16900 16920 16940 16960 16980 17000 17020 17040 17060 17080 17100 17120 17140 17160 17180 17200 17220 17240 17260 17280 17300 17320 17340 17360 17380 17400 17420 17440 17460 17480 17500 17520 17540 17560 17580 17600 17620 17640 17660 17680 17700 17720 17740 17760 17780 17800 17820 17840 17860 17880 17900 17920 17940 17960 17980 18000 18020 18040 18060 18080 18100 18120 18140 18160 18180 18200 18220 18240 18260 18280 18300 18320 18340 18360 18380 18400 18420 18440 18460 18480 18500 18520 18540 18560 18580 18600 18620 18640 18660 18680 18700 18720 18740 18760 18780 18800 18820 18840 18860 18880 18900 18920 18940 18960 18980 19000 19020 19040 19060 19080 19100 19120 19140 19160 19180 19200 19220 19240 19260 19280 19300 19320 19340 19360 19380 19400 19420 19440 19460 19480 19500 19520 19540 19560 19580 19600 19620 19640 19660 19680 19700 19720 19740 19760 19780 19800 19820 19840 19860 19880 19900 19920 19940 19960 19980 20000 20020 20040 20060 20080 20100 20120 20140 20160 20180 20200 20220 20240 20260 20280 20300 20320 20340 20360 20380 20400 20420 20440 20460 20480 20500 20520 20540 20560 20580 20600 20620 20640 20660 20680 20700 20720 20740 20760 20780 20800 20820 20840 20860 20880 20900 20920 20940 20960 20980 21000 21020 21040 21060 21080 21100 21120 21140 21160 21180 21200 21220 21240 21260 21280 21300 21320 21340 21360 21380 21400 21420 21440 21460 21480 21500 21520 21540 21560 21580 21600 21620 21640 21660 21680 21700 21720 21740 21760 21780 21800 21820 21840 21860 21880 21900 21920 21940 21960 21980 22000 22020 22040 22060 22080 22100 22120 22140 22160 22180 22200 22220 22240 22260 22280 22300 22320 22340 22360 22380 22400 22420 22440 22460 22480 22500 22520 22540 22560 22580 22600 22620 22640 22660 22680 22700 22720 22740 22760 22780 22800 22820 22840 22860 22880 22900 22920 22940 22960 22980 23000 23020 23040 23060 23080 23100 23120 23140 23160 23180 23200 23220 23240 23260 23280 23300 23320 23340 23360 23380 23400 23420 23440 23460 23480 23500 23520 23540 23560 23580 23600 23620 23640 23660 23680 23700 23720 23740 23760 23780 23800 23820 23840 23860 23880 23900 23920 23940 23960 23980 24000 24020 24040 24060 24080 24100 24120 24140 24160 24180 24200 24220 24240 24260 24280 24300 24320 24340 24360 24380 24400 24420 24440 24460 24480 24500 24520 24540 24560 24580 24600 24620 24640 24660 24680 24700 24720 24740 24760 24780 24800 24820 24840 24860 24880 24900 24920 24940 24960 24980 25000 25020 25040 25060 25080 25100 25120 25140 25160 25180 25200 25220 25240 25260 25280 25300 25320 25340 25360 25380 25400 25420 25440 25460 25480 25500 25520 25540 25560 25580 25600 25620 25640 25660 25680 25700 25720 25740 25760 25780 25800 25820 25840 25860 25880 25900 25920 25940 25960 25980 26000 26020 26040 26060 26080 26100 26120 26140 26160 26180 26200 26220 26240 26260 26280 26300 26320 26340 26360 26380 26400 26420 26440 26460 26480 26500 26520 26540 26560 26580 26600 26620 26640 26660 26680 26700 26720 26740 26760 26780 26800 26820 26840 26860 26880 26900 26920 26940 26960 26980 27000 27020 27040 27060 27080 27100 27120 27140 27160 27180 27200 27220 27240 27260 27280 27300 27320 27340 27360 27380 27400 27420 27440 27460 27480 27500 27520 27540 27560 27580 27600 27620 27640 27660 27680 27700 27720 27740 27760 27780 27800 27820 27840 27860 27880 27900 27920 27940 27960 27980 28000 28020 28040 28060 28080 28100 28120 28140 28160 28180 28200 28220 28240 28260 28280 28300 28320 28340 28360 28380 28400 28420 28440 28460 28480 28500 28520 28540 28560 28580 28600 28620 28640 28660 28680 28700 28720 28740 28760 28780 28800 28820 28840 28860 28880 28900 28920 28940 28960 28980 29000 29020 29040 29060 29080 29100 29120 29140 29160 29180 29200 29220 29240 29260 29280 29300 29320 29340 29360 29380 29400 29420 29440 29460 29480 29500 29520 29540 29560 29580 29600 29620 29640 29660 29680 29700 29720 29740 29760 29780 29800 29820 29840 29860 29880 29900 29920 29940 29960 29980 30000 30020 30040 30060 30080 30100 30120 30140 30160 30180 30200 30220 30240 30260 30280 30300 30320 30340 30360 30380 30400 30420 30440 30460 30480 30500 30520 30540 30560 30580 30600 30620 30640 30660 30680 30700 30720 30740 30760 30780 30800 30820 30840 30860 30880 30900 30920 30940 30960 30980 31000 31020 31040 31060 31080 31100 31120 31140 31160 31180 31200 31220 31240 31260 31280 31300 31320 31340 31360 31380 31400 31420 31440 31460 31480 31500 31520 31540 31560 31580 31600 31620 31640 31660 31680 31700 31720 31740 31760 31780 31800 31820 31840 31860 31880 31900 31920 31940 31960 31980 32000 32020 32040 32060 32080 32100 32120 32140 32160 32180 32200 32220 32240 32260 32280 32300 32320 32340 32360 32380 32400 32420 32440 32460 32480 32500 32520 32540 32560 32580 32600 32620 32640 32660 32680 32700 32720 32740 32760 32780 32800 32820 32840 32860 32880 32900 32920 32940 32960 32980 33000 33020 33040 33060 33080 33100 33120 33140 33160 33180 33200 33220 33240 33260 33280 33300 33320 33340 33360 33380 33400 33420 33440 33460 33480 33500 33520 33540 33560 33580 33600 33620 33640 33660 33680 33700 33720 33740 33760 33780 33800 33820 33840 33860 33880 33900 33920 33940 33960 33980 34000 34020 34040 34060 34080 34100 34120 34140 34160 34180 34200 34220 34240 34260 34280 34300 34320 34340 34360 34380 34400 34420 34440 34460 34480 34500 34520 34540 34560 34580 34600 34620 34640 34660 34680 34700 34720 34740 34760 34780 34800 34820 34840 34860 34880 34900 34920 34940 34960 34980 35000 35020 35040 35060 35080 35100 35120 35140 35160 35180 35200 35220 35240 35260 35280 35300 35320 35340 35360 35380 35400 35420 35440 35460 35480 35500 35520 35540 35560 35580 35600 35620 35640 35660 35680 35700 35720 35740 35760 35780 35800 35820 35840 35860 35880 35900 35920 35940 35960 35980 36000 36020 36040 36060 36080 36100 36120 36140 36160 36180 36200 36220 36240 36260 36280 36300 36320 36340 36360 36380 36400 36420 36440 36460 36480 36500 36520 36540 36560 36580 36600 36620 36640 36660 36680 36700 36720 36740 36760 36780 36800 36820 36840 36860 36880 36900 36920 36940 36960 36980 37000 37020 37040 37060 37080 37100 37120 37140 37160 37180 37200 37220 37240 37260 37280 37300 37320 37340 37360 37380 37400 37420 37440 37460 37480 37500 37520 37540 37560 37580 37600 37620 37640 37660 37680 37700 37720 37740 37760 37780 37800 37820 37840 37860 37880 37900 37920 37940 37960 37980 38000 38020 38040 38060 38080 38100 38120 38140 38160 38180 38200 38220 38240 38260 38280 38300 38320 38340 38360 38380 38400 38420 38440 38460 38480 38500 38520 38540 38560 38580 38600 38620 38640 38660 38680 38700 38720 38740 38760 38780 38800 38820 38840 38860 38880 38900 38920 38940 38960 38980 39000 39020 39040 39060 39080 39100 39120 39140 39160 39180 39200 39220 39240 39260 39280 39300 39320 39340 39360 39380 39400 39420 39440 39460 39480 39500 39520 39540 39560 39580 39600 39620 39640 39660 39680 39700 39720 39740 39760 39780 39800 39820 39840 39860 39880 39900 39920 39940 39960 39980 40000 40020 40040 40060 40080 40100 40120 40140 40160 40180 40200 40220 40240 40260 40280 40300 40320 40340 40360 40380 40400 40420 40440 40460 40480 40500 40520 40540 40560 40580 40600 40620 40640 40660 40680 40700 40720 40740 40760 40780 40800 40820 40840 40860 40880 40900 40920 40940 40960 40980 41000 41020 41040 41060 41080 41100 41120 41140 41160 41180 41200 41220 41240 41260 41280 41300 41320 41340 41360 41380 41400 41420 41440 41460 41480 41500 41520 41540 41560 41580 41600 41620 41640 41660 41680 41700 41720 41740 41760 41780 41800 41820 41840 41860 41880 41900 41920 41940 41960 41980 42000 42020 42040 42060 42080 42100 42120 42140 42160 42180 42200 42220 42240 42260 42280 42300 42320 42340 42360 42380 42400 42420 42440 42460 42480 42500 42520 42540 42560 42580 42600 42620 42640 42660 42680 42700 42720 42740 42760 42780 42800 42820 42840 42860 42880
```

[illegible]

00AM-78MS LGH JAF 78 J26000V17M
LJY0121.0
394 HA,UCO 37.3 14.7
CCL WLE 8A,BLE 279.0 27.
EAR VEL 8A,UCO 332.1 27.5
TMB 13.0

[illegible]

```

      1  171035+001      1  1 171035+001      1  1 171035+001
      2  2119700+003      2  1 171035+001      2  1 171035+001
      3  171035+001      3  1 171035+001      3  1 171035+001
      4  171035+001      4  1 171035+001      4  1 171035+001
      5  171035+001      5  1 171035+001      5  1 171035+001
      6  171035+001      6  1 171035+001      6  1 171035+001

```


[illegible]

21

[illegible]

[illegible]

23

The lower contour plot gives the mean velocity for all points in the sky. Since the I_{\max} position may not correspond to the highest velocity, the contour indicators can rise above "F".

The incoming interstellar wind direction (at infinity) relative to the solar system, the direction to the sun, and the earth velocity vector are indicated in the plots and given in the parameter lists. The parameters of the model for this display are chosen to be $v = 20 \text{ km s}^{-1}$, $T = 10,000\text{K}$, ionization loss rate at 1 a.u. = $6.8 \times 10^{-8} \text{ s}^{-1}$ and downstream direction $\alpha = 72^\circ$, $\delta = 18^\circ$, V_{BAR} is the mean thermal velocity. DOY is the day-of-year and TH is the upwind-sun-earth angle.

The pattern seen for day 21 is a reasonably well-defined primary intensity distribution centered at $\alpha 212$ and $\delta -10$ which is produced by the combination of 30 km s^{-1} earth orbital velocity and helium atoms being directed along hyperbolas roughly parallel to the earth velocity vector. A secondary pattern is centered at $\alpha 312$ and $\delta -26$, with peak intensity about a factor of 4 lower than the primary peak. The closest approach of the maximum particle flow to \underline{v}_E occurs around day 21 (closest approach of the "x" to the "+"). As the day-of-year increases, the intensity becomes more collimated, because the particle orbits are less dispersed by solar gravity. The absolute value of the peak intensity goes through a broad maximum around day 101 (see Figure 3). Throughout this period, the mean velocity in the direction of I_{\max} is in excess of 70 km s^{-1} , but begins to drop at day 121, reflecting the fact that \underline{v}_E is moving away from I_{\max} and that \underline{v} itself is lower

because of less gravitational acceleration. The secondary pattern has now become too weak to show up on the contours.

Into summer, the intensity pattern broadens and in late summer/early fall the earth is moving in roughly the same direction as the interstellar gas. The velocity of I_{\max} drops to less than 20 km s^{-1} . In the meantime, atoms on acute hyperbolas (the so-called secondary component) have become evident in the velocity contours again near v_F , since they have swung around the sun, gaining kinetic energy, and oppose the earth's motion. However, their intensity remains very low until day 221 when they appear on the contour plots as a small collimated beam. By day 301, the secondary component has become more intense than the primary component, which has spread out into a broad, diffuse pattern.

Throughout fall, the patterns of both components elongate and eventually merge together forming an asymmetric annulus. The asymmetry arises mainly due to the earth's velocity. A secondary cause of asymmetry occurs because the gas flow is not directed in the ecliptic plane. The closest approach of the earth to the downstream direction occurs on day 338 (about 5°). If the earth were motionless and exactly in the downstream direction, a symmetric annulus would be formed since the primary and secondary components are indistinguishable.

Around the beginning of the year, the annulus shrinks and separates into primary and secondary components again. Note that because the velocity distribution is modified Maxwell-Boltzmann the pattern is actually continuous across the sky throughout the year with primary peaks always present; however, often the secondary intensities (and

those in-between the primary and secondary) are just too weak to show up on the contour graphs, which are limited to 1% of I_{\max} .

The magnitudes, gradients, and positions of the intensity in the sky give sufficient information to uniquely determine the density, temperature, velocity, and ionization rate of interstellar helium. Direct measurement of the neutral particles eliminates an important uncertainty in the optical backscatter technique: the required knowledge of the solar 584A flux and its line profile.

IV. DETERMINATION OF GAS PARAMETERS

Synoptic studies of the intensity were performed to delineate its dependence on the input parameters. In this section, details of the studies are given.

1. Absolute Magnitude

Figure 3 summarizes the seasonal variation of I_{\max} and \bar{v} at I_{\max} . The switchover from primary to secondary components occurs around the middle of October. The best times to measure the magnitude of the intensity are winter and spring. Not only does the highest value occur then, but also the mean velocity is high, so that about 100 eV per atom is available to trigger a detector.

2. Direction of I_{\max}

The position in the sky of the maximum intensity is influenced by the earth's velocity and the magnitude and direction of the interstellar

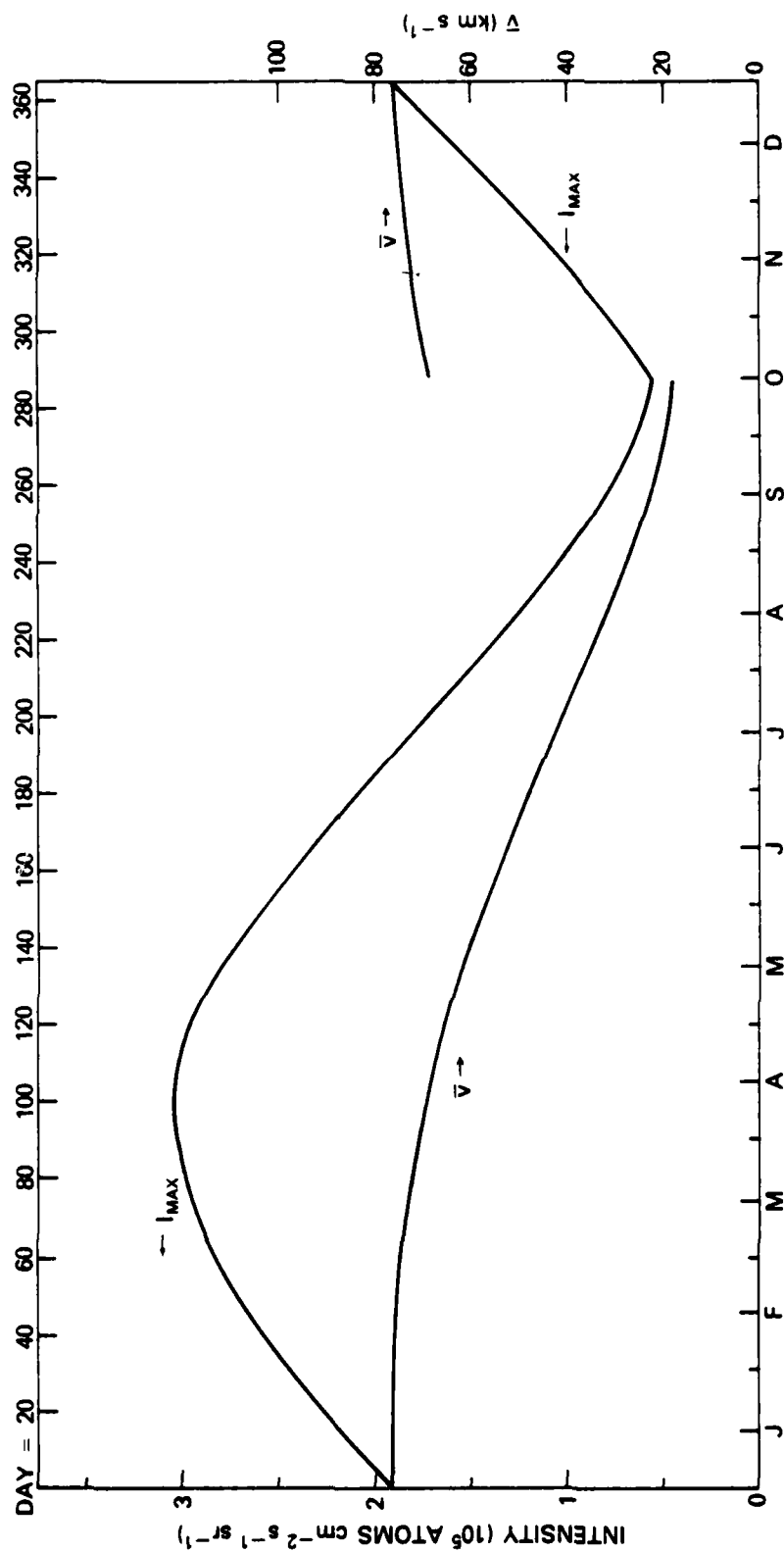


Fig. 3 — I_{max} (left axis) and v (right axis) vs. day-of-year (upper axis) and month (lower axis). The large tic marks on the lower axis are for the 15th day of each month and the small tics are the beginning of the month.

bulk flow velocity at infinity. Calculations have shown that near day 121 the position of I_{\max} is essentially independent of the magnitude of \underline{v} , so that a measurement on that date gives the direction of the incoming gas relative to the solar system. However, since the earth velocity is large and combined vectorially with the gas velocity, a change of 6° in the direction of \underline{v} translates to 3° in I_{\max} . Thus, to reduce the present uncertainty of $\pm 3^\circ$ in \underline{v} as determined optically (Weller and Meier, 1980) to, say, $\pm 1^\circ$, the precision in determining I_{\max} should be of the order of $\pm 0.5^\circ$.

At other times of year, the position of I_{\max} depends on $|\underline{v}|$ as well. Thus, if the direction of \underline{v} is known, $|\underline{v}|$ can be determined. For example, by changing $|\underline{v}|$ from 15 to 25 km s⁻¹ (but keeping the direction fixed), the position of I_{\max} shifts by 7° in the sky on day 1, and by a similar amount on day 300. Thus, the magnitude of the bulk flow velocity vector can be determined from position observations at different times of year, independent of instrument calibration.

3. Pattern Size: T and v Dependence

During the spring and summer, the width of the intensity pattern depends both upon temperature and $|\underline{v}|$. During periods when primary and secondary components are competing, the ionization rate also influences the pattern. However, since the ionization regime is about 0.5 a.u. in the upstream direction, β has little effect there.

Figure 4 shows a plot of I versus right ascension for the declination which includes I_{\max} , on day 60. Curves for three velocities and three temperatures are shown. It is clear that with a single

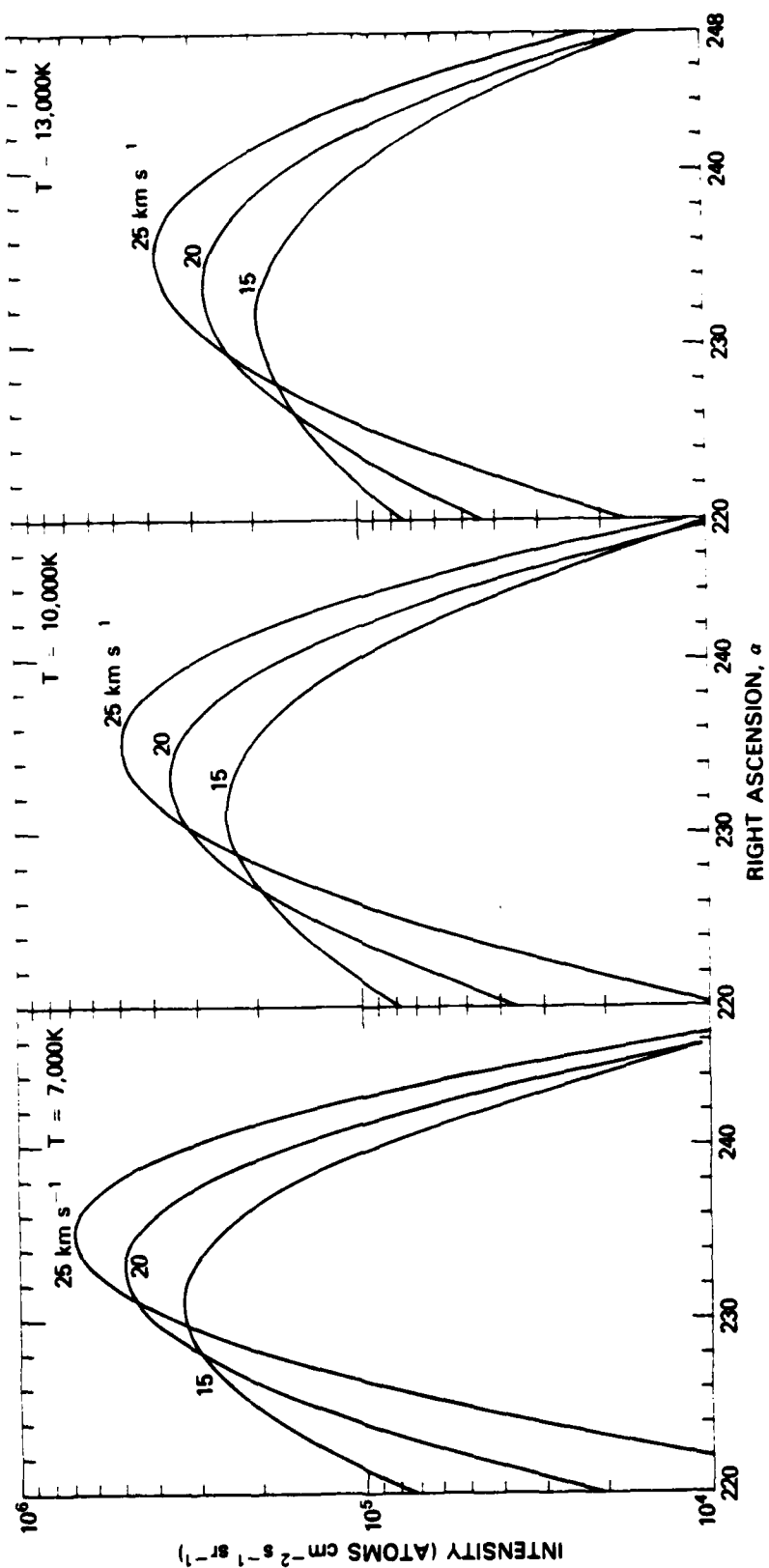


Fig. 4 — Intensity curves vs. right ascension for various velocities and temperatures for day 60. The declination in each case was chosen to pass through I_{max}

measurement, it is impossible to separate the influence of T from $|v|$. For example, $T = 13,000\text{K}$ and $v = 25 \text{ km s}^{-1}$ give the same intensity shape as $10,000\text{K}$ and 20 km s^{-1} . By making measurements at other times of year, the patterns show slightly different T and v dependences, but they are not likely to be distinguishable experimentally. As noted earlier, $|v|$ can be found if the gas direction is known. Thus, knowing the velocity, the temperature can be found from model calculations such as those in Figure 4, but measurement accuracy should be better than 1° .

4. Pattern Size: β Dependence

Photoionization of helium affects those intensities which are made up of atoms which have passed close to the sun. An example of this is shown in Figure 5 for day 301. In Figure 5a, primary and secondary components are seen for $\beta = 6.8 \times 10^{-8} \text{ s}^{-1}$. The secondary component is more intense with $I_{\text{max}} = 1.31 \times 10^5 \text{ cm}^{-2} \text{ s}^{-1} \text{ sr}^{-1}$. The primary component is more than a factor of two lower. Increasing β to $1.36 \times 10^{-7} \text{ s}^{-1}$ causes the maximum intensity to drop to $4.60 \times 10^4 \text{ cm}^{-2} \text{ s}^{-1} \text{ sr}^{-1}$ with the primary and secondary peak being nearly equal in magnitude. However, the primary component has broadened somewhat. Since the contours on the individual plots are normalized to each I_{max} , the broadening is relative to I_{max} . In effect what has happened in 5b is that the overall magnitudes of I have dropped as well as a lessening of the gradient across the primary peak. Also, since β does not affect spring or summer intensities, the "upstream to downstream" intensity ratio is quite sensitive to the photoionization rate.

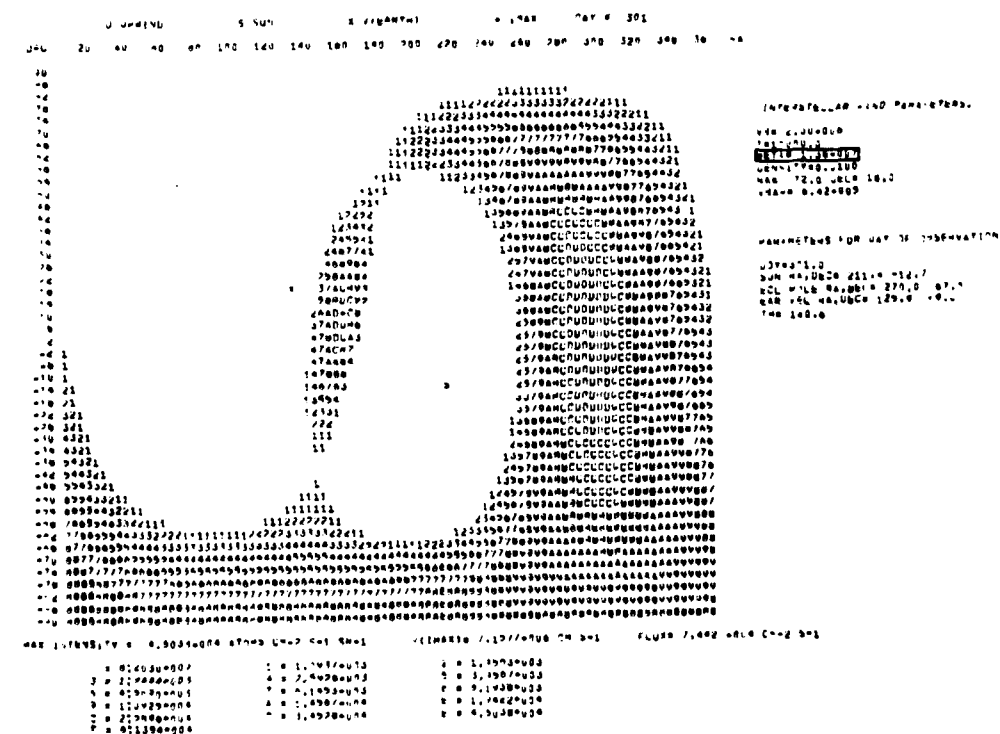
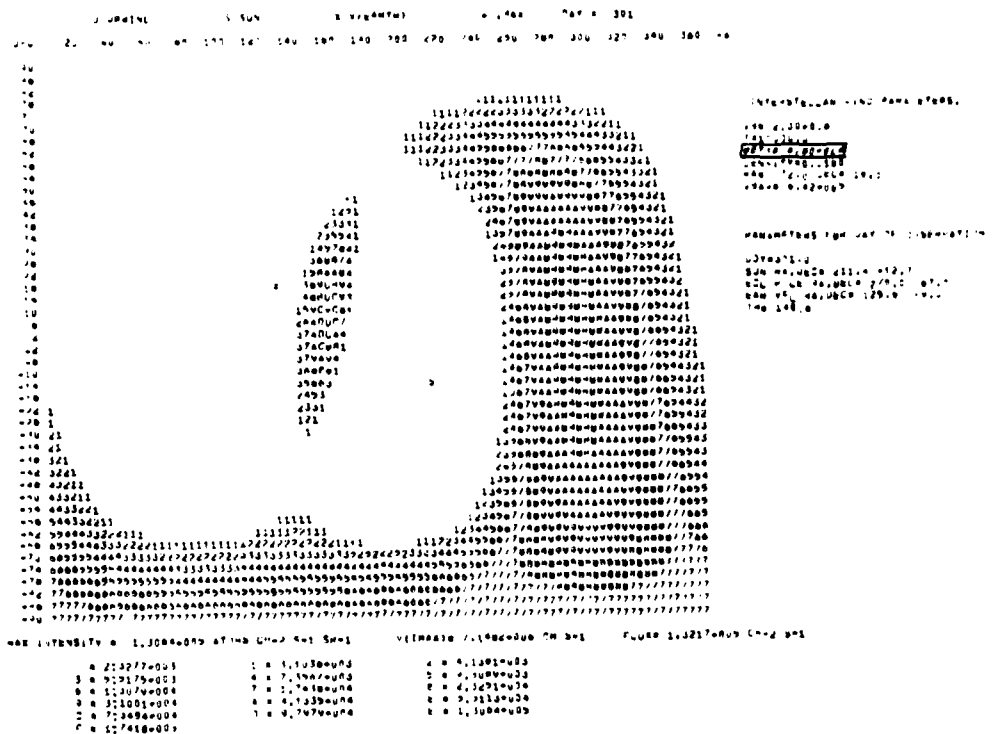


Fig. 5 — Comparison of intensity patterns on day 301 for $\beta = 6.8 \times 10^{-7} \text{ s}^{-1}$ (upper) and $\beta = 13.6 \times 10^{-7} \text{ s}^{-1}$ (lower)

Thus β influences the primary to secondary intensity ratios as well as the size and magnitudes of the patterns (especially in the fall), and is quite sensitive to the intensity relative to other times of year.

V. SUMMARY

It is clear from the discussion above that observations from the earth of the interstellar atomic helium intensity pattern can yield the density, temperature, velocity, and photoionization rate. Observations must be made at three different times of year to delineate all of the parameters. The angular resolution must be $< 1^\circ$ for accurate spatial determination. However, an instrument with a well-known angular response could be used, even if its field of view is larger than 1° .

Several other caveats are important in considering neutral particle measurements. The experiment must be well above the atmosphere so that collisions do not degrade the incoming beam. Estimates of the effect are very uncertain, since the $\text{He} + \text{O}$ differential cross section is not known (especially at small angles). Estimates using a $\text{He} + \text{Ar}$ cross section indicate that the observing platform should be above 450-500 km to avoid significant perturbation of the incoming He. Another effect which may cause minor degradation of the beam is focusing by the earth's gravitational field (Fahr et al., 1976). However, for observations in the direction of the incoming helium this effect is negligible.

ACKNOWLEDGMENTS

I would like to thank N. R. Linder for computational assistance.

REFERENCES

- Fahr, H. J., Lay, G., and Blum, P. W., 1976, Astron. Astrophys.,
52, 363.
- Holzer, T. E., 1977, Rev. Geophys. Sp. Phys., 15, 467.
- Meier, R. R., 1977, Astron. Astrophys., 55, 211.
- Thomas, G. E., 1978, Ann. Rev. Earth Planet. Sci., 6, 173.
- Weller, C. S., and Meier, R. R., 1974, Astrophys. J., 193, 471.
- Weller, C. S., and Meier, R. R., 1980, Astrophys. J., submitted
for publication.

DATE
FILMED
- 8